Heliyon 10 (2024) e28162

Contents lists available at ScienceDirect

Heliyon

journal homepage: www.cell.com/heliyon

Research article

ADCY4 promotes brain metastasis in small cell lung cancer and is associated with energy metabolism

Yidan Sun [a,1], Yixun Chen [b,1], Xin Zhang [a], Dan Yi [a], Fanming Kong [a], Linlin Zhao [a], Dongying Liao [a], Lei Chen [a], Qianqian Ma [c,**], Ziheng Wang [d,e,*]

[a] Department of Oncology, First Teaching Hospital of Tianjin University of Traditional Chinese Medicine, Tianjin, 300382, China
[b] Research Center of Clinical Medicine, Affiliated Hospital of Nantong University, Nantong, Jiangsu, China
[c] Affiliated Women's Hospital of Jiangnan University Wuxi, Jiangsu, China
[d] Centre for Precision Medicine Research and Training, Faculty of Health Sciences, University of Macau, Macau SAR, China
[e] Department of Clinical Bio-bank, Affiliated Hospital of Nantong University, Jiangsu, China

ARTICLE INFO

Keywords:
ADCY4
SCLC
BMs
Mfuzz
WGCNA
Anti-PD1

ABSTRACT

Brain metastasis (BMs) in small cell lung cancer (SCLC) has a very poor prognosis. This study combined WGCNA with the mfuzz algorithm to identify potential biomarkers in the peripheral blood of patients with BMs. By comparing the significantly differentially expressed genes present in BMs samples, we identified ADCY4 as a target for further study. Expression of ADCY4 was used to cluster mfuzz expression pattern, and 28 hub genes for functional enrichment. PPI network analysis were obtained by comparing with differentially expressed genes in BMs. GABRE, NFE4 and LMOD2 are highly expressed in patients with BMs and have a good diagnostic effect. Immunoinfiltration analysis showed that SCLC patients with BMs may be associated with memory B cells, Tregs, NK cell activation, macrophage M0 and dendritic cell activation. prophytic was used to investigate the ADCY4-mediated anti-tumor drug response. In conclusion, ADCY4 can be used as a promising candidate biomarker for predicting BMs, molecular and immune features in SCLC. PCR showed that ADCY4 expression was increased in NCI–H209 and NCI–H526 SCLC cell lines. In vitro experiments confirmed that the expression of ADCY4 was significantly decreased after anti-PD1 antibody treatment, while the expression of energy metabolism factors were significantly different. This study reveals a potential mechanism by which ADCY4 mediates poor prognosis through energy metabolism -related pathways in SCLC.

1. Introduction

Small cell lung cancer (SCLC) accounts for 15%–20% of lung cancer [1], when they are found, and the prognosis is poor [2,3]. The brain is the most common and most dangerous site for metastasis in patients with SCLC, and is an important cause of death from SCLC. According to statistics, about 15% of patients with SCLC have brain metastasis(BMs) at first diagnosis. The median survival time of patients with BMs is only 4–6 months in the era of chemoradiotherapy for SCLC.In recent years [4], with the development of

* Corresponding authorCentre for Precision Medicine Research and Training, Faculty of Health Sciences, University of Macau, Macau SAR, China
** Corresponding author. Affiliated Women's Hospital of Jiangnan University Wuxi, Jiangsu, China.
E-mail addresses: 9862023234@jiangnan.edu.cn (Q. Ma), wang.ziheng@connect.um.edu.mo (Z. Wang).
[1] These authors contributed equally.

https://doi.org/10.1016/j.heliyon.2024.e28162
Received 17 October 2023; Received in revised form 29 February 2024; Accepted 13 March 2024
Available online 28 March 2024

immunotherapy mode, the survival of BMs patients has been improved. However, since the mechanism of BMs in SCLC has not been fully defined, the treatment is still one of the major challenges affecting the quality of life and survival of SCLC patients [1,5,6]. It is very important to prevent and predict BMs. Malignant tumor cells use free fatty acids and ketones released by neighboring catabolic cells to produce energy [7], which can also be achieved through energy metabolism in the TCA cycle. Targeting energy metabolic pathways in cancer may be an effective cancer treatment strategy [8]. A large number of studies have confirmed the relevant mechanisms of action between how tumor metastases respond to and adapt to the tissue and biochemical environment [9].

GSE161968 is a dataset of patients with BMs in SCLC(https://www.ncbi.nlm.nih.gov/gds). We identified DEGs associated with BMs. Then, the modules most associated with BMs and the genes related to energy metabolism were selected and intersected with DEGs. Utilizing the R software package "WGCNA," a gene co-expression network was established. Subsequently, an adjacency matrix was generated to depict the correlation strength among the nodes. The transformation of the adjacency matrix into a topological overlay matrix (TOM) was carried out in this investigation, followed by hierarchical clustering for the recognition of modules, each consisting of no less than 30 genes. Ultimately, the identification of feature genes, hierarchical clustering modules, and the amalgamation of comparable modules were executed (abline = 0.25). The red, violet and grey modules that may be most relevant to the mechanism related to the occurrence of BMs were obtained for WGCNA. the red module most significantly associated with BMs, to explore the potential molecular mechanisms and predictive value of energy metabolic pathways for BMs risk in patients with SCLC.

By comparing the significantly differentially expressed genes present in BMs samples, we identified ADCY4 as a target for further study. Expression of ADCY4 was used for mfuzz expression pattern clustering, and expression of ADCY4 was used for mfuzz expression pattern clustering, a total of 50 clusters were obtained, and cluster 22 with the strongest significance and correlation was selected for analysis. By comparing 577 ADCY4-related genes contained in cluster 22 with differentially expressed genes in BMs. What's more, GABRE, NFE4 and LMOD2 are highly expressed in patients with BMs and have good diagnostic efficacy. In the BMs group, the infiltration difference of immune cells, such as memory B cells, Tregs, NK cellsactivated, Macrophages M0 and Dendritic cellsactivated was significantly higher, which may suggested that in SCLC patients with BMs, These immune cells may be activated. However, whether this difference has clinical prognostic significance needs to be verified with a large number of samples. The expression difference was evaluated by batch ROC and batch box diagram. Furthermore, drug response prediction was carried out utilizing pRRophetic. In order to explore the ADCY4-mediated response of tumor cells to drug therapy, we found that expression of ADCY4 is correlated with the apoptosis-inducing OSU-03012. Anti-mutant cell proliferation Tipifarnib, a variety of VEGF receptor tyrosine kinase inhibitors, PARP inhibitors, and some chemotherapy drugs were significantly related to sensitivity.

2. Materials and methods

2.1. Data processing

The gene expression files were collected from the GSE161968 in the Gene Expression Omnibus (GEO) [10]. GPL20115 [Agilent-067406 Human CBC lncRNA + mRNA microarray V4.0 (Probe name version)] was used to extract expression profile information. The dataset included mRNA microarray assay data of peripheral blood mononuclear cells from 12 patients (6 patients with BMsBMs and 6 patients without BMsBMs) to standardize and normalize gene expression profiles.

2.2. Identification of significant modules

First, we evaluated the availability of differentially expressed genes related to energy metabolism and constructed a gene co-expression network using an R software package named "WGCNA". An adjacency matrix is created to depict the correlation strength. The TOM is used to quantitatively represent the resemblance between two nodes through assessing their weighted correlation with other nodes. Subsequently, hierarchical clustering is executed to detect clusters, with each cluster comprising a minimum of 30 genes (minModuleSize = 30). Lastly, feature genes are determined, modules are hierarchically clustered, and alike modules are combined (abline = 0.25).

The module for co-expression consists of a group of genes that exhibit significant similarity in topological overlap. Genes within a specific module typically demonstrate increased levels of co-expression. In this investigation, we employed two different approaches to pinpoint the critical modules associated with clinical characteristics. The eigengene of the module (referred to as ME) serves as a representation of the expression profile for the module within individual samples. Module membership (MM) denotes the correlation coefficient between genes and module eigengenes, providing insight into the trustworthiness of genes categorized within a particular module.

2.3. Gene Ontology (GO) enrichment analysis

In order to further reveal the biological significance of the six stem cell-related marker models, a large-scale functional enrichment study of genes in different dimensions and levels was conducted through Gene Ontology (GO) enrichment analysis [11]. KEGG (Kyoto Encyclopedia of Genes and Genomes) is a widely used database that stores information about genomes, biological pathways, diseases, and drugs [12]. All significantly differentially expressed genes were annotated with GO function using the R package clusterprofiler to identify significantly enriched biological processes. The enrichment results were visualized using the R package GOplot.

2.4. Analysis of immune infiltration

R-package cibersort evaluated the infiltration level of immune cells [13,14]. The result is visualized with the R package ggplot2.

2.5. Drug sensitivity prediction

Pharmacogenomic data from the Cancer Drug Sensitivity Genomics (GDSC) database were used to predict drug sensitivity in enrolled glioma cases. The semi-maximum inhibitory concentration (IC50) value was calculated by prophytic package to reflect the drug response [15].

2.6. Cell culture and drug treatment

BEAS-2B, NCI–H209 and NCI–H526 cells were purchased from Beijing Bena Institute of Biotechnology (Beijing, China). Cells were cultured in Gibco DEME F-12 medium with 10% FBS (Thermo Fisher, USA) at 37 °C with 5% CO2. For anti-PD-1 treatment (Bioxcell, SIM0010).

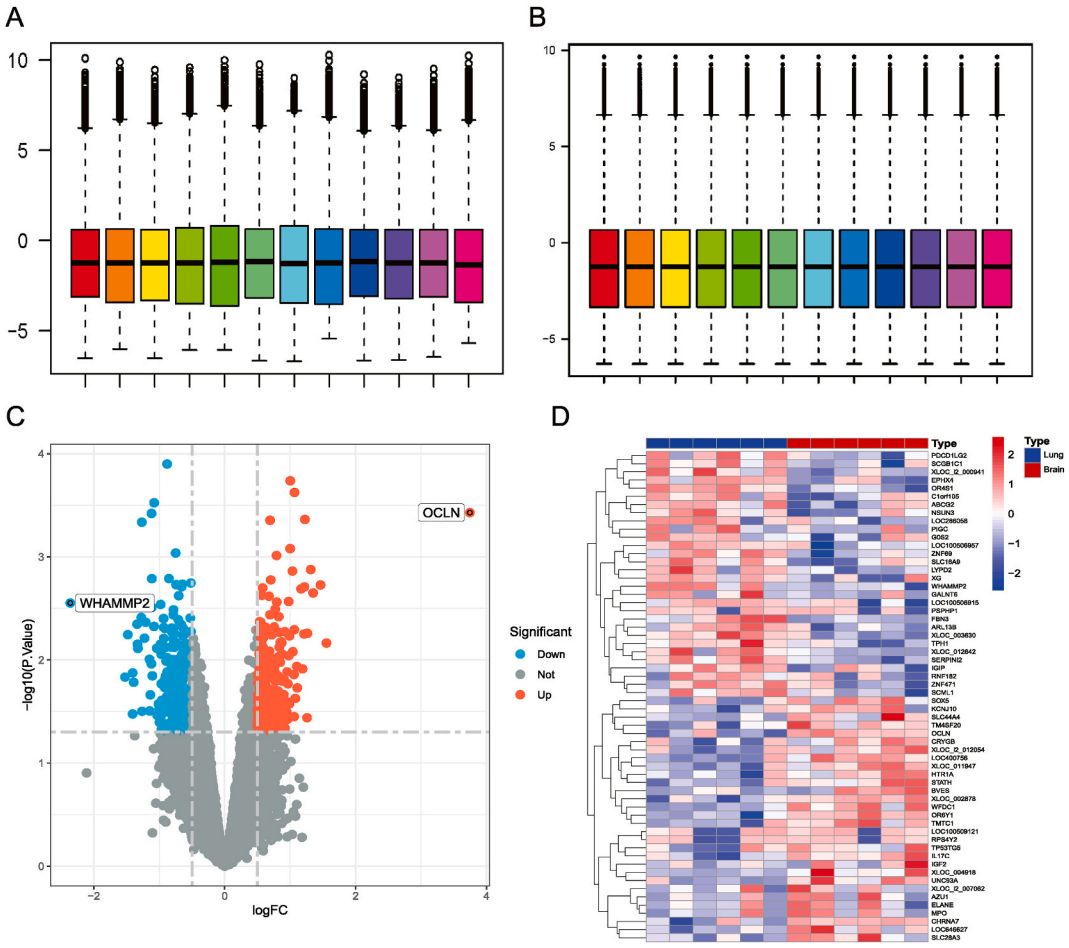

Fig. 1. (A) Comparison of the original data of mRNA microarray detection of peripheral blood mononuclear cells in 6 patients with BMs and 6 patients without BMs in the GSE161968 dataset; (B) Comparative box plots of standardized and normalized gene expression profiles of samples; (C) Volcano maps of differentially expressed genes between patients with BMs and patients without BMs in the GSE161968 dataset, with marked differences in energy metabolist-related genes; (D) Significantly differentially expressed genes related to energy metabolism between patients with BMs and patients without BMs in the GSE161968 dataset.

2.7. Quantitative real-time polymerase chain reaction (qRT-PCR)

TRIzol reagent was employed for the extraction of total RNA from BEAS-2B, NCI–H209, and NCI–H526 cell lines (Thermo Fisher, USA). The HiScript II SuperMix (Vazyme, China) was utilized to generate cDNA from 500 ng of RNA. The qRT-PCR was conducted in the ABI 7500 System (Thermo Fisher, USA) with the SYBR Green Master Mix. The PCR amplification conditions included 45 cycles of 94 °C for 10 min, followed by 94 °C for 10 s, and 60 °C for 45 s each. GAPDH acted as the internal reference The following is a list of the

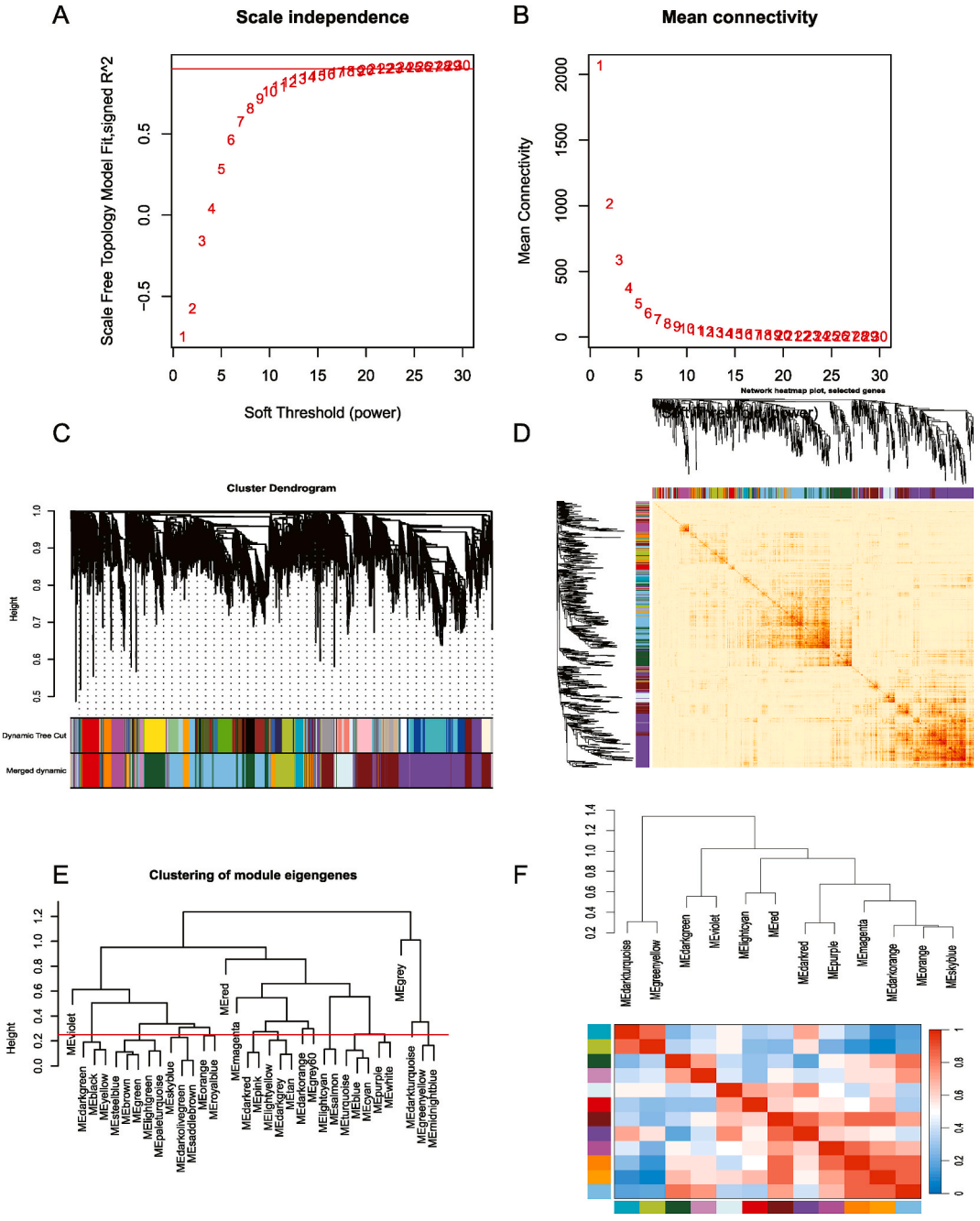

Fig. 2. WGCNA screens Hub genes.(A) scale-free index analysis of each soft threshold power (β); (B) Average connectivity analysis for each soft threshold power; (C) The clustering tree of the sample, the tree of all differentially expressed genes is based on the measurement clustering of dissimilarity (1-TOM), and the ribbon shows the results of automatic single-block analysis; (D) Clustering correlation heat maps of samples; (E) Clustering of samples; (F) Heat maps of correlation of module characteristic genes in each sample.

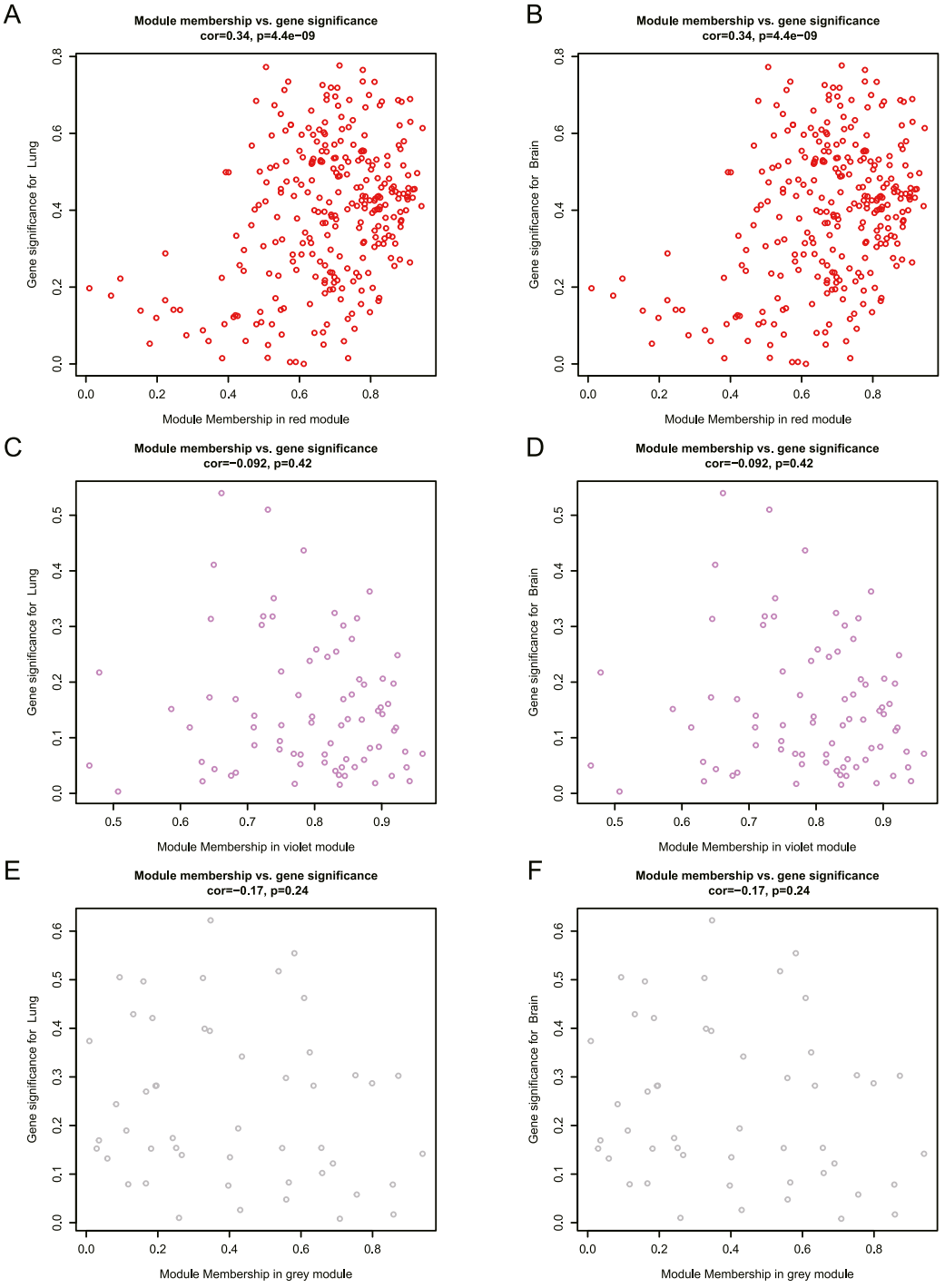

Fig. 3. Screening of the most relevant modules of BMs. (A–B) Scatter plot of correlation between the weighted scores of genes in the red module and their significance respectively in samples without BMs and BMs; (C–D) Scatter plot of correlation between the weighted scores of genes in the violet module and their significance respectively in samples without BMs and BMs; (E–F) Scatter plot of correlation between the weighted scores of genes in the grey module and their significance respectively in samples without BMs and BMs. (For interpretation of the references to colour in this figure legend, the reader is referred to the Web version of this article.)

sequences of primer pairs for the genes that were being targeted.

Gene	Forward primer sequence (5′-3′)	Reverse primer sequence (5′-3′)
ADCY4	GAGCCTACCTATCTGGTCATCG	GACTCCAGGTAACGGGTCATCA
E-cad	CGAGAGCTACACGTTCACGG	GGGTGTCGAGGGAAAAATAGG
N-cad	TCAGGCGTCTGTAGAGGCTT	ATGCACATCCTTCGATAAGACTG
VIM	GACGCCATCAACACCGAGTT	CTTTGTCGTTGGTTAGCTGGT
FN1	AAGAAGGGCTCGTGTGACAG	TCTTGTCCTACATTCGGCGG
BCL-2	ATCGCCCTGTGGATGACTGAGT	GCCAGGAGAAATCAAACAGAGGC
BAX	TCAGGATGCGTCCACCAAGAAG	TGTGTCCACGGCGGCAATCATC
CASP3	GGAAGCGAATCAATGGACTCTGG	GCATCGACATCTGTACCAGACC
CASP9	GTTTGAGGACCTTCGACCAGCT	CAACGTACCAGGAGCCACTCTT
GAPDH	CTGGGCTACACTGAGCACC	AAGTGGTCGTTGAGGGCAATG

2.8. Cell viability

Cell viability was assessed by the Cell Counting Kit-8 method (Beyotime, China). The CCK-8 solution was administered at specified time intervals. Following a 2-h incubation at 37 °C, the optical density at 450 nm for each well was measured using a microplate reader.

2.9. Statistical analysis

Excel (Microsoft) and R software (version 4.0.2) were utilized to perform all data processing and analysis. When comparing two sets of continuous variables, the statistical significance of variables distributed normally was calculated using an independent chi-square test or Fisher's exact test. For the analysis of the statistical significance between two sets of categorical variables, the chi-square test or Fisher's exact test was applied. All P values were considered statistically significant if they were less than 0.05 and were two-sided.

3. Results

3.1. Screening of hub genes in energy metabolism

To investigate the value of energy metabolism pathway in predicting the risk of BMs (BMs) in patients with SCLC (SCLC). We obtained mRNA microarray detection data of peripheral blood mononuclear cells from 12 GSE161968 disease datasets (6 patients with BMs and 6 patients without BMs) from GEO, and standardized and normalized gene expression profiles (Fig. 1A and B). The volcano

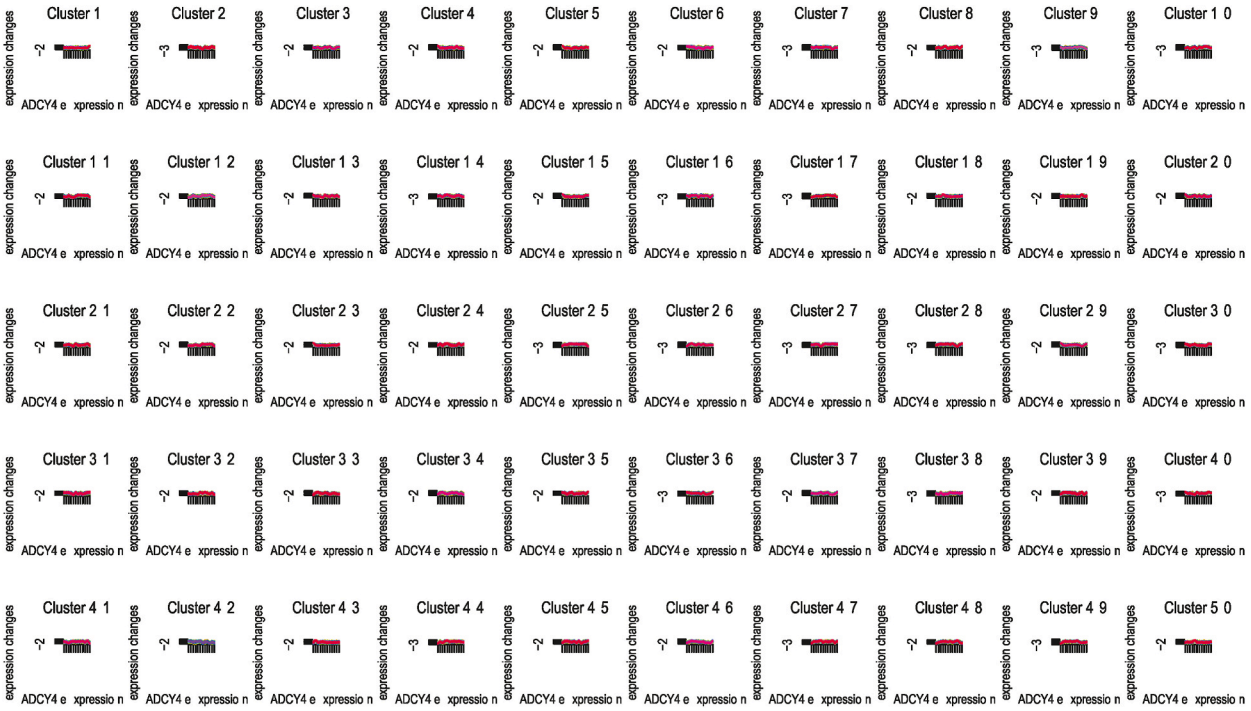

Fig. 4. Cluster analysis of mfuzz expression patterns was performed according to the expression level of ADCY4.

map (Fig. 1C) and heat map (Fig. 1D) showed the DEGs in the GSE161968 dataset.

3.2. Co-expression network analysis

The weighted gene co-expression network analysis was used to identify hub genes. Upon sample clustering, no abnormal data points were identified. To establish a scale-free network, the scale-free fit index was set to 0.9, leading to the determination of a minimum soft threshold of 9 (Fig. 2A). Furthermore, modules with a feature factor exceeding 0.75 were consolidated into two modules (Fig. 2B). The module membership (MM) reflects the association between gene expression values and characteristic genes within a module. To enhance the screening process, modules exhibiting a feature factor greater than 0.75 were merged into multiple modules (Fig. 2C). GS indicates the correlation between the module gene and the sample. The modules were associated with clinical features by calculating MM and GS values. The 283 potential targets most associated with BMs in the red module (Fig. 2D).

We also show correlations between each sample and weighted co-expression modules in order to screen out the modules most closely associated with the occurrence of BMs. The clustering grouping of weighted coexpression modules (Fig. 2E) and the correlation between modules (Fig. 2F) were confirmed by the tree diagram.

We further analyzed the Top 3 significant clusters associated with the occurrence of BMs obtained by WGCNA, including red, violet, and grey. In this three module, the scatter plots of correlation between membership and gene expression of SCLC without BMs (Fig. 3A–C, E) and those with BMs (Fig. 3B–D, F) respectively show that the red module(cor = 0.34, p = 4.4e−09) is the most significant, suggesting that the genes contained in this module are most relevant to the potential mechanism of BMs in SCLC.

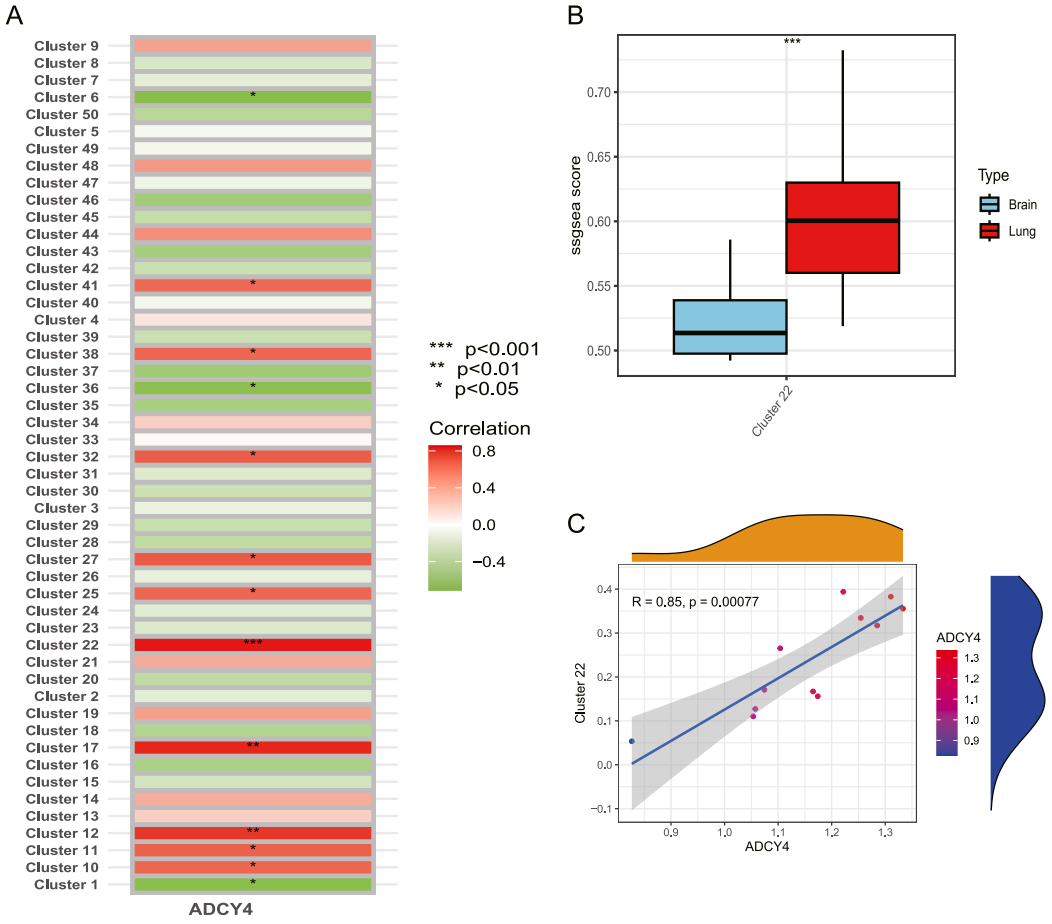

Fig. 5. Correlation analysis between ssGSEA expression pattern clustering and ADCY4 expression. (A) The significance of expression pattern clustering calculated by Ssgsea and the correlation between cluster scores and ADCY4 expression (sorted by number of genes); (B) The score comparison of expression pattern Cluster with Cluster 22 showed significant difference in the presence or absence of BMs, and the correlation was strongest; (C) Scatter plots of correlation between different clustering patterns and ADCY4 expression levels.

3.3. Cluster analysis of mfuzz expression pattern

WGCNA was carried out based on energy metabolism-related genes, and the red group was the most significantly related to energy metabolism. DEGs detected in lung tumor tissue and BMs tumor tissue, and ADCY4 was selected as the object of further study. We conducted cluster analysis of mfuzz expression pattern according to the expression level of ADCY4. Fig. 4 shows the sample

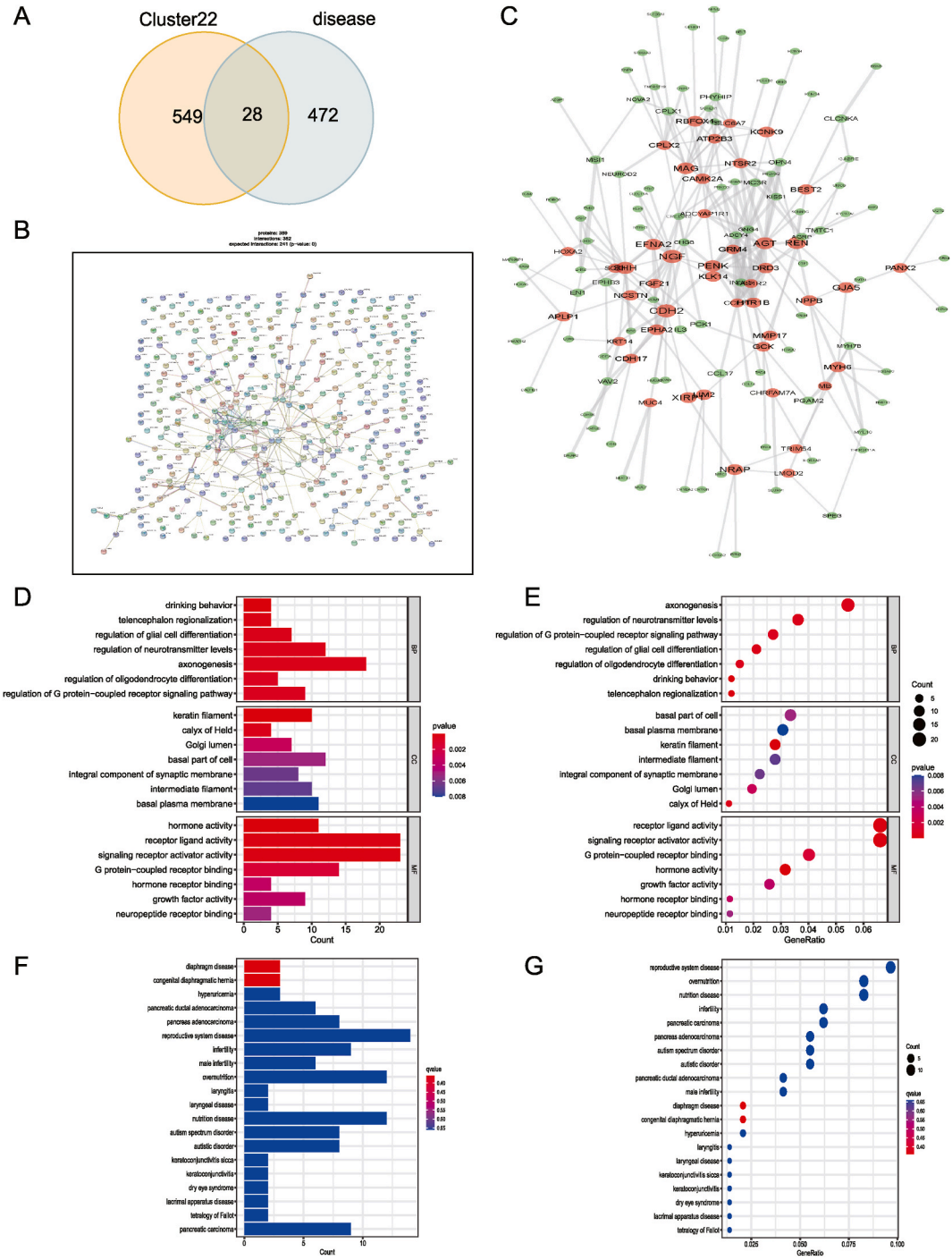

Fig. 6. Enrichment analysis. (A) Venn diagram of intersection between genes of ADCY4 cluster 22 and differential genes related to BMs; (B) Hub components of Cluster 22 intermolecular interaction networks among ensemble genes; intermolecular interaction networks. (C–D) Bar and bubble graphs for GO enrichment analysis of 28 ADCY4-related genes; (E–F) DO enrichment analysis of 28 ADCY4-related genes, bar and bubble graphs.

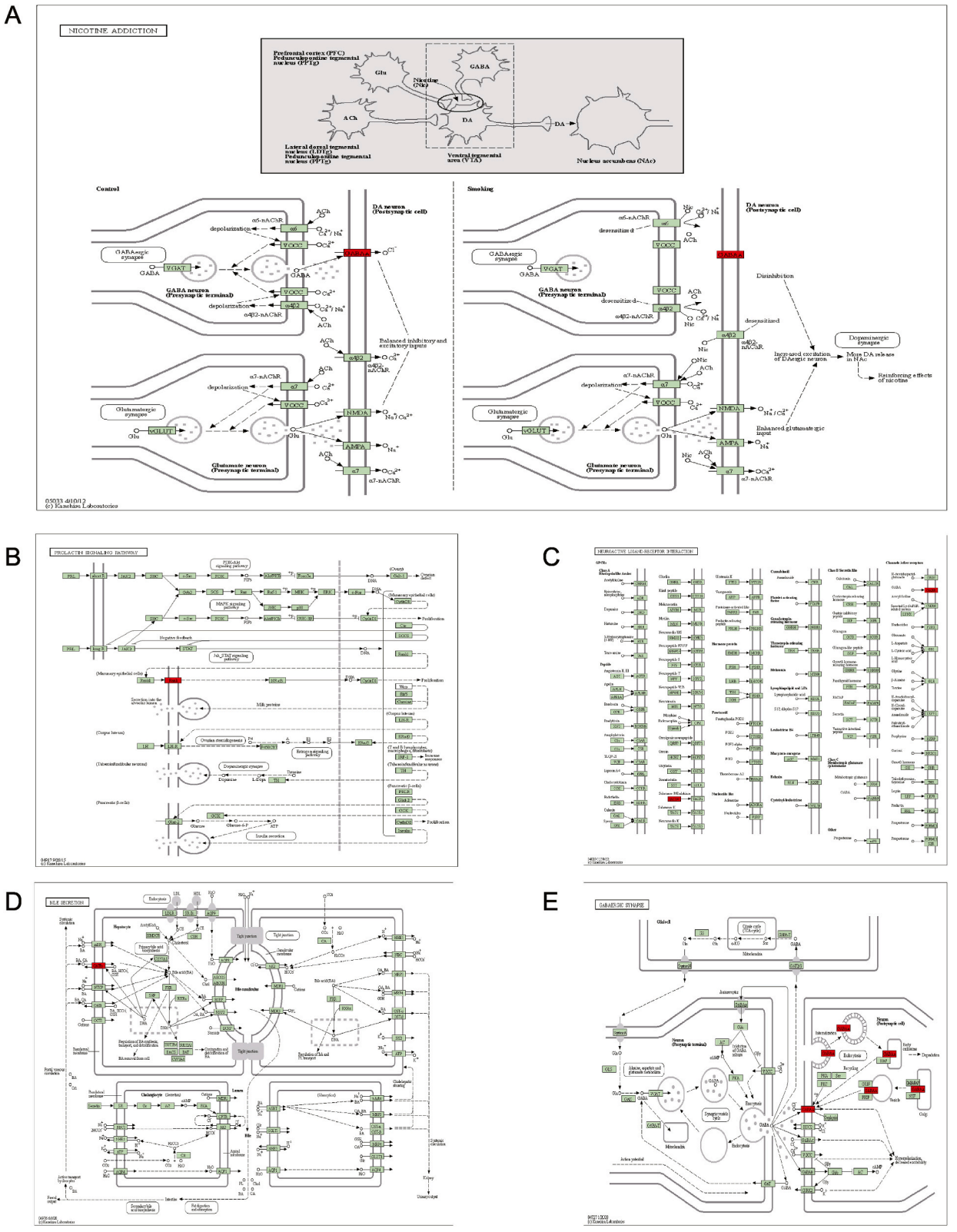

Fig. 7. Pathway enrichment map of KEGG enrichment analysis of 28 AdCy4-related genes. (A) Nicotine addiction pathway enrichment map. (B) Prolactin signaling pathway; (C) Enrichment map of Neuroactive ligand-receptor interaction pathway; (D) Concentration map of Bile secretion pathway. (E) Concentration map of GABAergic synapse pathway.

classification among 50 cluster groups. Sequencing by number of genes showed the correlation between significance and cluster scores and ADCY4 expression (Fig. 5A). After comparison, Cluster 22 was found to have a significant difference in the presence or absence of BMs between groups, and the strongest correlation. The differences are shown in a box diagram (Fig. 5B). The scatter plot showed the correlation between the score of Cluster 22 expression pattern and the expression of ADCY4 (Fig. 5C).

3.4. Enrichment analysis

In order to further explore whether ADCY4 is related to energy metabolism in the formation of BMs, we took the intersection of genes in cluster 22 and differential genes related to BMs(Fig. 6A). We screened Hub genes to construct intermolecular interaction networks to understand the associations (Fig. 6B).

We obtained 28 hub ADCY4-related energy metabolism genes and enriched them with GO and DO. Functional enrichment analysis showed that cell components were enriched in activity, receptor ligand activity signaling receptor activator activity. biology process was significantly enriched in drinking behavior and telencephalon regionalization(Fig. 6D and E). It is suggested that regulatory mechanism correlation with the energy metabolism genes closely related to ADCY4 may affect the intercellular interactions and

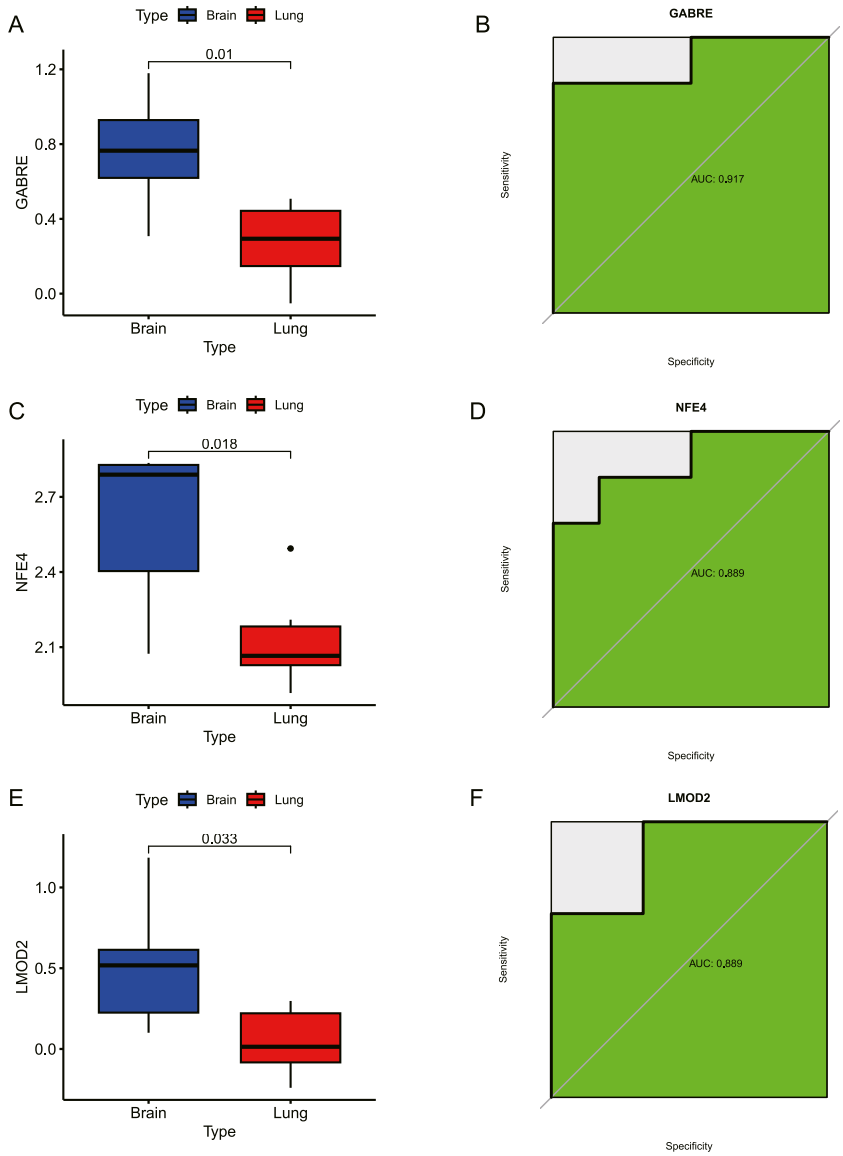

Fig. 8. Difference analysis and efficacy verification of 28 ADCY4-related genes on BMs; (A–B) GABRE was highly expressed in patients with BMs and had good diagnostic efficacy (AUC = 0.917). (C–D) NFE4 was highly expressed in patients with BMs and had good diagnostic efficacy (AUC = 0.889). (E-F)LMOD2 was highly expressed in patients with BMs and had good diagnostic efficacy (AUC = 0.889).

molecules such as hormone activity and drinking behavior. Cytokeratin has been reported to play a guiding role in bone, brain and soft tissue metastases in a variety of cancers. The expression was different in primary and metastatic cancer specimens [16]. Enrichment analysis of disease annotation(DO) found that hub energy metabolism genes closely related to ADCY4 were enriched in pancreatic adenocarcinoma, nutritional diseases, heart dysfunction related diseases, reproductive system diseases, hypogonadism, and pervasive developmental disorders (Fig. 6E and F). This suggests that there may be a potential mechanism link between BMs of SCLC and related diseases affected by the above energy metabolic pathways.

In KOBAS, KEGG enrichment analysis demonstrated molecular mechanisms of potential action on 28 ADCY4-related genes. For example, Nicotine addiction(Fig. 7A), Prolactin signaling pathway (Fig. 7B); Neuroactive ligand-receptor interaction(Fig. 7C); Bile secretion (Fig. 7D). GABAergic synapse pathway enrichment map (Fig. 7E).

3.5. Efficacy evaluation of hub genes

Among the 28 ADCY4-related genes, GABRE, NFE4 and LMOD2 have selective expression differences in BMs, and they are highly expressed in BMs patients. ROC curve verified that GABRE (AUC = 0.917) (Fig. 8A and B), NFE4 (AUC = 0.889) (Fig. 8C and D), LMOD2 (AUC = 0.889) (Fig. 8E and F) had good differential efficacy for BMs. Although there is no data to confirm the effect of NFE4 on tumor progression, database-based bioinformatics analyses have found that NFE4 has potential prognostic significance for cancers such as renal clear cell carcinoma [17].

3.6. Immunoinfiltration correlation of ADCY4 clustering

Next, we studied the relationship between CIBERSORT deconvolution algorithm ADCY4 and immunity. We showed the accumulation bar graph of the degree of infiltration of immune cells in each sample in the GSE161968 (Fig. 9A). Although the difference in

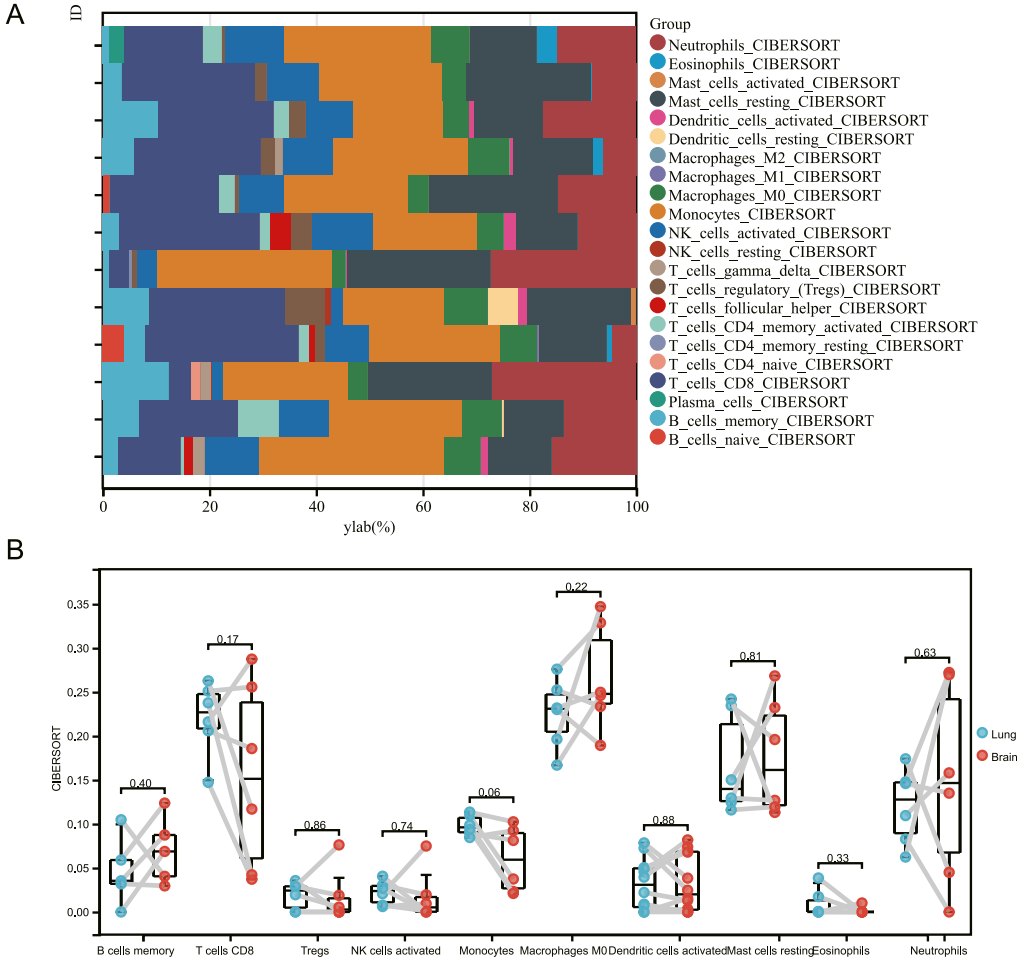

Fig. 9. Relationship between ADCY4 and immunity. (A) Cumulative bar chart of the degree of infiltration of immune cells in each sample in the GSE161968 dataset; (B) Differences in infiltration of immune cells in the BMs group in the GSE161968 dataset.

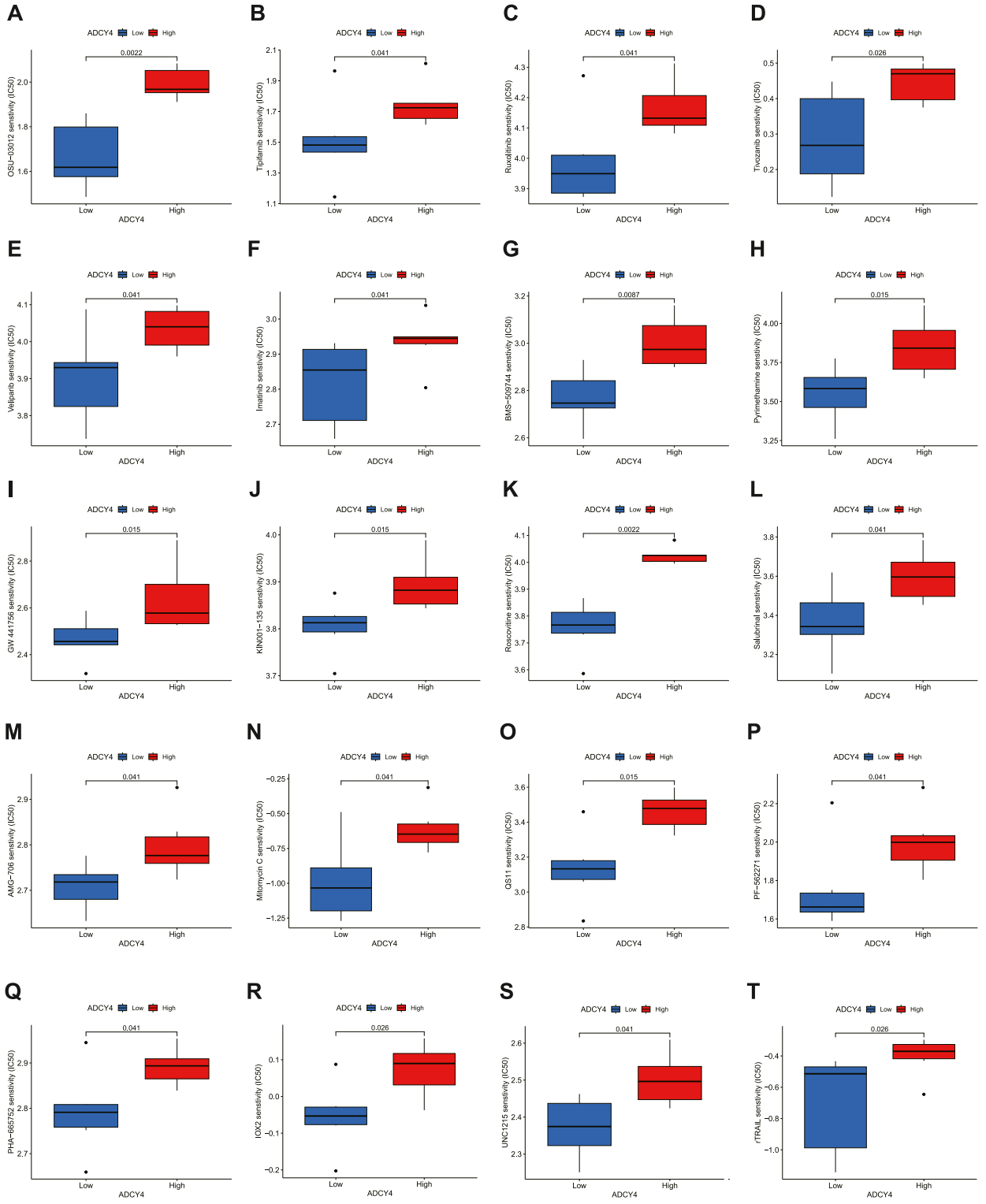

Fig. 10. Drug sensitivity analysis of ADCY4. Drug sensitivity difference between high and low ADCY4 expression groups. OSU-03012(A)、Tipifarnib (B)、Ruxolitinib(C)、Tivozanib(D)、Veliparib(E)、Imatinib(F)、BMs-509744(G)、Pyrimethamine(H)、GW 441756(I)、KIN001-135(J)、Roscovitine (K)、Salubrinal(L)、AMG-706(M)、Mitomycin C(N)、QS11(O)、PF-562271(P)、PHA-665752(Q)、IOX2(R)、UNC1215(S)、rTRAIL(T).

infiltration of immune cells in the BMs group was not statistically significant due to the small sample size of the control group, there were still significant differences between the groups. However, the activation of memory B cells, Tregs, NK cellsactivated, Macrophages M0 and Dendritic cells was significantly higher, which may suggest that these immune cells may be activated in SCLC patients with BMs. However, whether this difference has clinical prognostic significance needs to be verified with a large number of samples (Fig. 9B).

3.7. Validation of the relationship between ADCY4 expression level and drug sensitivity

We further evaluated whether ADCY4 mediated the response of tumor cells to drug treatment. We found and analyzed that there was a statistically significant relationship between ADCY4 expression level and the following drug sensitivity. OSU-03012 (Fig. 10A) induces apoptosis of PC-3 cells. Tipifarnib (Fig. 10B), a specific farnesyltransferase (FTase) inhibitor, acts on H-ras or N-ras mutant cells and has the most significant anti-proliferation effect. Ruxolitinib (Fig. 10C) is a kinase inhibitor that inhibits Janus-associated kinases (JAKs) JAK1 and JAK2, mediating several cytokine and growth factor signaling important for hematopoietic and immune function. Tivozanib (Fig. 10D) and AMG-706(Fig.10 M) are inhibitors of VEGF receptor tyrosine kinase. Veliparib (Fig. 10E) is a novel PARP inhibitor. BMs-509744 (Fig. 10G) is a potent and selective inhibitor of interleukin-2 induced T cell kinase (ITK). Imatinib (Fig. 10F), Pyrimethamine (Fig. 10H), Mitomycin C (Fig.10 N), GW 441756 (Fig. 10I) were TRKA inhibitors. KIN001-135 (Fig. 10J) is a treatment for multiple Omicronine variants, Roscovitine (Fig. 10K) is a CDK inhibitor, and Salubrinal (Fig.10L) is a potentially useful reagent for

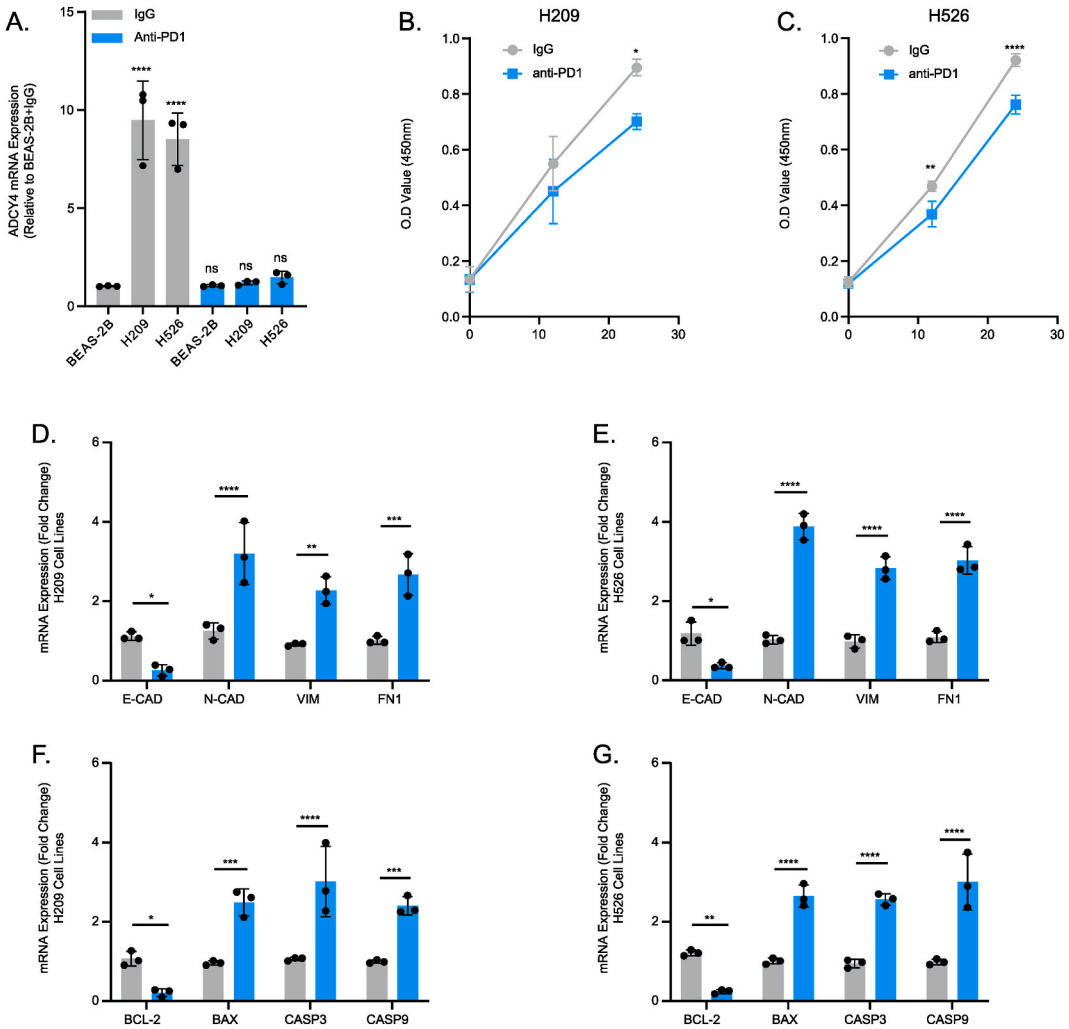

Fig. 11. Anti-PD-1 therapy inhibits progression of small cell lung cancer. (A) Expression of ADCY4 in BEAS-2B, NCI–H209 and NCI–H526 cell lines before and after anti-PD1 treatment. (B–C) Changes in cell viability in NCI–H209 and NCI–H526 cell lines before and after anti-PD1 treatment. (D–E) Changes in energy metabolism makers in NCI–H209 and NCI–H526 cell lines before and after anti-PD1 treatment. (F–G) Changes in apoptotic makers in NCI–H209 and NCI–H526 cell lines before and after anti-PD1 treatment. N = 3/group. *≤0.05, **≤0.01 , ***≤0.001 , ****≤0.0001. The results are presented as mean ± SEM.

studying the mechanisms of endoplasmic reticulum stress-induced apoptosis. QS11 (Fig.10O) is a potent, ATP-competitive, reversible inhibitor of FAK. PF-562271(Fig.10P) is also a FAK inhibitor, and PHA-665752 (Fig.10Q) is a c-Met inhibitor. IOX2 (Fig.10R) is an HIF/HIF PHD inhibitor. UNC1215 (Fig. 10S) is a malignant glioma antagonist. rTRAIL (Fig.10T) is a recombinant human tumor necrosis factor-associated apoptosis-inducing ligand variant.

3.8. Anti-PD-1 therapy inhibits progression of SCLC

The results of PCR showed that ADCY4 expression was elevated in SCLC cell lines NCI–H209 and NCI–H526, and that ADCY4 expression was significantly decreased in SCLC cell lines after treatment with anti-PD1 antibody (Fig. 11A). Meanwhile, cell viability of NCI–H209 and NCI–H526 cell lines were significantly decreased after anti-PD1 antibody treatment (Fig. 11B and C). We then examined the expression of energy metabolism makers in SCLC cells after anti-PD1 treatment. After treatment with PD1, E-CAD expression decreased, while N-CAD, VIM and FN1 expression increased (Fig. 11D and E). We also found that anti-PD1 treatment promoted the expression of apoptotic makers in SCLC cell lines, as evidenced by a decrease in BCL-2 and an increase in BAX, CASP3 and CASP9 (Fig. 11F and G).

4. Discussion

The prognosis of patients with SCLC is very poor, and the 5-year survival rate is less than 5% [18–20]. BMs is the most common secondary metastasis of SCLC, and it is also the most important factor in the progression of the disease [21–23]. According to statistics, BMs in patients with SCLC are an important cause of death. Clustering of mfuzz expression patterns and functional analysis of optimal diagnostic biomarkers were explored. In this study, we combined WGCNA with the mfuzz algorithm to identify potential biomarkers in the peripheral blood of patients with BMs. Firstly, we constructed a gene co-expression network using R software package "WGCNA". In addition, modules with a feature factor greater than 0.75 (set the minimum number of genes in the module to 30) are combined into multiple modules for screening. Then we construct an adjacency matrix to describe the strength of the correlation. In our study, we convert the adjacency matrix into a topological overlay matrix (TOM), performing hierarchical clustering to identify modules, each containing at least 30 genes. Finally, we compute the feature genes, hierarchical clustering modules, and merge similar modules (abline = 0.25). The red, violet and grey modules that may be most relevant to the mechanism related to the occurrence of BMs were obtained for WGCNA. We evaluated the availability of differentially expressed genes related to energy metabolism, the red module most significantly associated with BMs, to explore the potential molecular mechanisms and predictive value of energy metabolic pathways for BMs risk in patients with SCLC.

In this study, WGCNA was combined with the mfuzz algorithm to identify potential biomarkers in the peripheral blood of patients with BMs, thereby screening for ADCY4. By comparing the significantly differentially expressed genes present in BMs samples, we identified ADCY4 as a target for further study. ADCY4 is a protein-coding gene associated with diseases such as adenoma, thyroid adenoma, male precocious puberty and chondrodysplasia, and is functionally associated with perturbation of adenylate cyclase activity, alcohol and opioid addiction. A number of studies have confirmed that ADCY4 is significantly down-regulated in breast cancer and other cancers, which is related to promoter hypermethylation, and is closely related to the survival rate of patients with different tumor subtypes and tumor stages [11,24,25]. ADCY4 acts as a direct mechanism to avoid excessive inflammatory responses during cytoplasmic lipopolysaccharide (LPS) activation of non-classical caspase-11-dependent inflammasome processes [26]. ADCY4 is also enriched in the inflammatory mediators regulatory pathway of transient receptor potential (TRP) channels [27]. Including ADORA2B-mediated anti-inflammatory cytokine production and β-2 adrenergic dependent CFTR expression. Gene ontology (GO) annotations associated with this gene include phosphoxylyase activity and adenylate cyclase activity [28]. The protein expressed by ADCY4 may be involved in the development of lung tumors associated with inflammation through purine metabolism [29].

In our study, ADCY4 expression level from GSE161968 was used for mfuzz pattern clustering, a total of 50 clusters were obtained, and Cluster 22 with the strongest significance and correlation was selected for analysis. By comparing 577 ADCY4-related genes contained in cluster 22 with differentially expressed genes in BMs, we obtained a total of 28 hub genes for functional enrichment and PPI network analysis. The expression difference was evaluated by batch ROC and batch box diagram. To further explore the functional enrichment of 28 hub genes in ADCY4 during BMs formation. It was found that most of the related genes were concentrated in keratin fibers, and the molecular function was significantly correlated with the activity of receptor ligand and signal receptor activator. It is suggested that the regulatory mechanism of energy metabolism genes closely related to ADCY4 may affect cellular interaction, hormone activity, drinking behavior, etc. It is also significantly enriched in pancreatic adenocarcinoma, nutritional diseases, heart dysfunction related diseases, reproductive system diseases, hypogonadism, and pervasive developmental disorders. It is suggested that there may be a potential mechanism relationship between BMs of SCLC and related diseases influenced by the above energy metabolic pathways.

Overall, WGCNA was combined with the mfuzz algorithm to identify potential biomarkers in the peripheral blood of patients with BMs, thereby screening for ADCY4. We investigated the potential application of ADCY4 in the prediction of BMs in SCLC through bioinformatics. Drug sensitivity analysis for ADCY4 may contribute to the development of new tumor treatment strategies. In addition, the level of immune cell infiltration of ADCY4 in the microenvironment of BMs in SCLC can guide whether patients should undergo immunotherapy or targeted therapy, providing patients with a personalized treatment plan and improving patient survival and quality of life.

PCR showed that ADCY4 expression was increased in NCI–H209 and NCI–H526 SCLC cell lines. In vitro experiments confirmed that the expression of ADCY4 was significantly decreased after anti-PD1 antibody treatment, while the expression of energy metabolism

factors were significantly different. In vitro experiments revealed that after anti-PD1 antibody treatment, the expression of ADCY4 increased, while the expression of E-CAD decreased, and the expression of N-CAD, VIM and FN1 increased. In addition, the expression of apoptosis factor BCL-2 decreased, and the expression of BAX, CASP3 and CASP9 increased. These results suggest a potential mechanism by which ADCY4 mediates poor prognosis in SCLC via energy metabolism -related pathways. However, the direct molecular mechanism of ADCY4 mediating poor prognosis in SCLC needs to be further verified in vivo and in vitro.

Ethical approval

As a public database, TCGA and GEO has received the necessary ethical approvals. The public data we collect from it complies with all applicable laws, regulations, and policies for the protection of human subjects.

Funding

This artical was supported by Tianjin Municipal Education Commission Scientific Research project (2019KJ051) and Wuxi Medical Development Branch (Obstetrics and Gynecology, FZXK2021008).

Data availability statement

All data can be accessed vis correspondence authors.

CRediT authorship contribution statement

Yidan Sun: Writing – original draft, Software, Resources, Formal analysis, Data curation. **Yixun Chen:** Writing – review & editing, Writing – original draft, Formal analysis, Data curation, Conceptualization. **Xin Zhang:** Funding acquisition. **Dan Yi:** Conceptualization. **Fanming Kong:** Writing – review & editing, Supervision. **Linlin Zhao:** Investigation, Data curation. **Dongying Liao:** Investigation. **Lei Chen:** Writing – review & editing. **Qianqian Ma:** Writing – original draft, Validation, Resources, Data curation. **Ziheng Wang:** Writing – original draft, Validation.

Declaration of competing interest

The authors declare that they have no known competing financial interests or personal relationships that could have appeared to influence the work reported in this paper.

Acknowledgment

Not applicable.

References

[1] S. A, Controversies in the treatment of advanced stages of small cell lung cancer, Front. Radiat. Ther. Oncol. 42 (2010) 193–197, https://doi.org/10.1159/000262476. Epub 2009 Nov, (- 0071-9676 (Print)): p. - 193-197.
[2] K, G., et al., - Combined Chemotherapy with Cisplatin, Etoposide, and Irinotecan versus Topotecan.
[3] M. Xingjun, et al., Paclitaxel combined with ticagrelor inhibits B16F10 and lewis lung carcinoma cell metastasis, Oncologie 24 (2) (2022) 283–294.
[4] P. Pm, et al., - Treatment of brain metastases in small cell lung cancer: decision-making amongst, Radiother. Oncol. 149 (2020 Aug) 84–88, https://doi.org/10.1016/j.radonc.2020.04.015. Epub 2020, (- 1879-0887 (Electronic)): p. - 84-88.
[5] H. Mm, et al., - Asymptomatic brain metastases (BM) in small cell lung cancer (SCLC): MR-imaging, J. Neuro Oncol. 48 (3) (2000 Jul) 243–248, https://doi.org/10.1023/a:1006427407281 (- 0167-594X (Print)): p. - 243-8.
[6] Z.H. Wang, et al., Effect of region on the outcome of patients receiving PD-1/PD-L1 inhibitors for advanced cancer, Int. Immunopharm. 74 (2019).
[7] C. E, et al., Cellular fatty acid metabolism and cancer, - Cell Metab 18 (2) (2013 Aug 6) 153–161, https://doi.org/10.1016/j.cmet.2013.05.017. Epub 2013, (- 1932-7420 (Electronic)): p. - 153-61.
[8] M.-P. M, et al., The role of lipids in cancer progression and metastasis, Cell Metab. 34 (11) (2022 Nov 1) 1675–1699, https://doi.org/10.1016/j.cmet.2022.09.023. Epub, (- 1932-7420 (Electronic)): p. - 1675-1699.
[9] B. F, et al., Oxidative metabolism drives immortalization of neural stem cells during, Cell 182 (6) (2020 Sep 17) 1490–1507.e19, https://doi.org/10.1016/j.cell.2020.07.039. Epub, (- 1097-4172 (Electronic)): p. - 1490-1507.e19.
[10] L. J, et al., Downregulation of lncRNA XR_429159.1 linked to brain metastasis in patients with, Front. Oncol. 11 (2021 May 17) 603271, https://doi.org/10.3389/fonc.2021.603271 eCollection, (- 2234-943X (Print)): p. - 603271.
[11] F. Y, et al., Epigenetic identification of ADCY4 as a biomarker for breast cancer: an, Epigenomics 11 (14) (2019 Nov) 1561–1579, https://doi.org/10.2217/epi-2019-0207. Epub 2019 Oct, (- 1750-192X (Electronic)): p. - 1561-1579.
[12] O. H, et al., KEGG: kyoto Encyclopedia of genes and genomes, Nucleic Acids Res. 27 (1) (1999 Jan 1) 29–34, https://doi.org/10.1093/nar/27.1.29 (- 0305-1048 (Print)): p. - 29-34.
[13] C. B, et al., - profiling tumor infiltrating immune cells with CIBERSORT, Methods Mol. Biol. 1711 (2018) 243–259, https://doi.org/10.1007/978-1-4939-7493-1_12, 1940-6029 (Electronic)): p. - 243-259.
[14] N. Am, et al., - Robust enumeration of cell subsets from tissue expression profiles, Nat. Methods 12 (5) (2015 May) 453–457, https://doi.org/10.1038/nmeth.3337. Epub 2015 Mar 30., (- 1548-7105 (Electronic)): p. - 453-7.
[15] G. P, C. N, H. Rs, pRRophetic: an R package for prediction of clinical chemotherapeutic response, PLoS One 9 (9) (2014 Sep 17) e107468, https://doi.org/10.1371/journal.pone.0107468 (- 1932-6203 (Electronic)): p. - e107468.

[16] L. Q, et al., - Keratin 13 expression reprograms bone and brain metastases of human prostate, Oncotarget 7 (51) (2016 Dec 20) 84645–84657, https://doi.org/10.18632/oncotarget.13175 (- 1949-2553 (Electronic)): p. - 84645-84657.
[17] P. Q, et al., - identification of a 5-gene signature predicting progression and prognosis of, Med Sci Monit 25 (2019 Jun 13) 4401–4413, https://doi.org/10.12659/MSM.917399 (- 1643-3750 (Electronic)): p. - 4401-4413.
[18] K. Gp, et al., Small cell lung cancer, J Natl Compr Canc Netw 11 (1) (2013 Jan 1) 78–98, https://doi.org/10.6004/jnccn.2013.0011 (- 1540-1413 (Electronic)): p. - 78-98.
[19] T. LA, S. Rl, J. A, Lung cancer statistics, Adv. Exp. Med. Biol. 893 (2016) 1–19, https://doi.org/10.1007/978-3-319-24223-1_1 (- 0065-2598 (Print)): p. - 1-19.
[20] Y.D. Sun, et al., Low expression of RGL4 is associated with a poor prognosis and immune infiltration in lung adenocarcinoma patients, Int. Immunopharm. 83 (2020).
[21] S. Te, G. Em, Limited-stage small cell lung cancer: current chemoradiotherapy treatment, Oncol. 15 (2) (2010) 187–195, https://doi.org/10.1634/theoncologist.2009-0298. Epub 2010, (- 1549-490X (Electronic)): p. - 187-95.
[22] D. Ik, V. Ky, v.M. Jp, Treatment of extensive-stage small cell lung carcinoma: current status and future, Eur. Respir. J. 35 (1) (2010 Jan) 202–215, https://doi.org/10.1183/09031936.00105009 (- 1399-3003 (Electronic)): p. - 202-15.
[23] Z. Lingyan, et al., Glycoprofiling of early non-small cell lung cancer using lectin microarray technology, Oncologie 25 (5) (2023) 469–480.
[24] M. Xh, et al., - Identification of differentially methylated genes as diagnostic and prognostic, World J. Surg. Oncol. 19 (1) (2021 Jan 26) 29, https://doi.org/10.1186/s12957-021-02124-6 (- 1477-7819 (Electronic)): p. - 29.
[25] Y. Y, T. X, Analysis of genes associated with prognosis of lung adenocarcinoma based on GEO, Medicine (Baltim.) 99 (19) (2020 May) e20183, https://doi.org/10.1097/MD.0000000000020183 (- 1536-5964 (Electronic)): p. - e20183.
[26] C. R, et al., cAMP metabolism controls caspase-11 inflammasome activation and pyroptosis in, Sci. Adv. 5 (5) (2019 May 22) eaav5562, https://doi.org/10.1126/sciadv.aav5562 eCollection 2019, (- 2375-2548 (Electronic)): p. - eaav5562.
[27] H. K, et al., A novel tree shrew model of chronic experimental autoimmune uveitis and its, Front. Immunol. 13 (2022 May 27) 889596, https://doi.org/10.3389/fimmu.2022.889596 eCollection, (- 1664-3224 (Electronic)): p. - 889596.
[28] M. P, et al., - Lung proteomics combined with metabolomics reveals molecular characteristics of, Environ. Toxicol. 38 (12) (2023 Dec) 2915–2925, https://doi.org/10.1002/tox.23926. Epub 2023 Aug, (- 1522-7278 (Electronic)): p. - 2915-2925.
[29] F.-R. Mm, et al., Illuminating (HTLV-1)-induced adult T-cell leukemia/lymphoma transcriptomic, Virus Res. 338 (2023 Dec) 199237, https://doi.org/10.1016/j.virusres.2023.199237. Epub 2023, (- 1872-7492 (Electronic)): p. - 199237.